2026 IEEE International Conference on Robotics and Automation (ICRA 2026)
June 1-5, 2026. Vienna, Austria

TriCoSphere: A High-Dexterity, Large-Volume, 3-Finger Coaxial Spherical Manipulator

Runze Hu, Zhengying Zhu†, Jinyu Li†, Yatao Leng, Jingshuai Liu, and Chenxi Xiao*

***Abstract*— Designing robotic manipulators often requires balancing dexterity, speed, and payload capacity. While traditional serial-link and cable-driven manipulators offer high dexterity, they struggle to concurrently achieve high speed, and often lack the strength and stiffness required for many applications. To address these limitations, we present TriCoSphere, a novel 12-degree-of-freedom, three-fingered manipulator designed to optimize all three attributes. Each 4-DoF finger employs a Coaxial Spherical Parallel Mechanism (CSPM), which positions all actuators at the base. This parallel architecture minimizes finger inertia for high-speed motion and distributes loads across multiple linkages, enhancing payload capacity. We provide a complete kinematic analysis and develop an efficient inverse kinematics solver for precise fingertip control. Experiments demonstrate that each finger can support a 4.1 kg payload and achieve a motion bandwidth of 6.5 Hz. The manipulator's grasp range and dexterity are showcased by handling objects from a 20 mm sphere to a 300 mm acrylic ball, as well as performing complex in-hand manipulation tasks. TriCoSphere is cost-effective, robust, and open-sourced to support future research.**

I. Introduction

As robotics transitions from structured industrial environments to dynamic human-centric settings, the development of versatile and capable manipulators has been a long-standing objective in the field [1], [2], [3], [4]. In such contexts, a single robotic system may need to delicately handle a fragile object such as a slice of bread, then immediately switch to firmly grasping a heavy tool [5], [6], [7]. These rapid shifts in task demands impose inherently conflicting requirements on the manipulator: high DoFs for dexterity, low inertia for speed and responsiveness, and high structural stiffness for payload capacity [8]. Moreover, these attributes must often be realized within compact form factors [9], [10], and with robust performance in unstructured, unpredictable environments. Balancing these competing factors remains a central challenge in robotic hand design, calling for novel architectures capable of delivering strength, agility, and precision within a single integrated system [11].

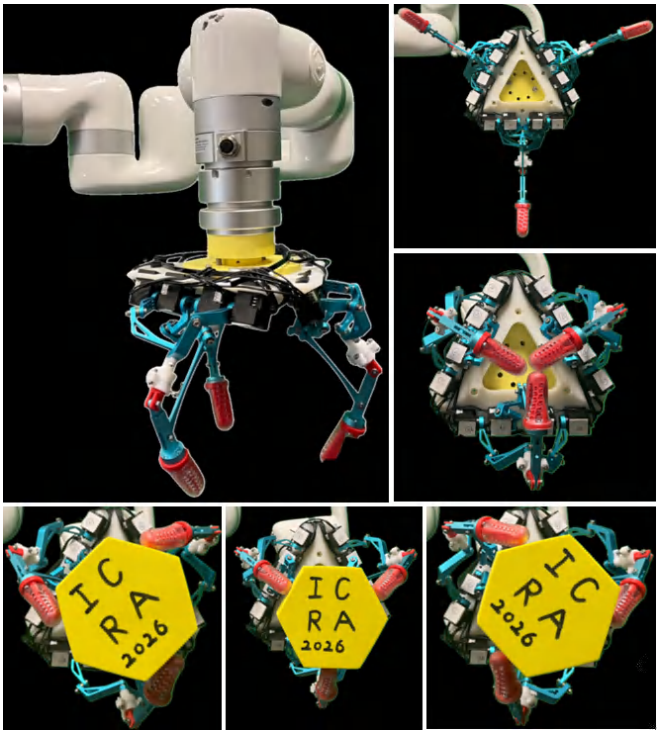

Fig. 1: The TriCoSphere manipulator. Its novel 4-DoF parallel-kinematic fingers offer low inertia, a large grasping volume, and high payload capabilities.

Current approaches to dexterous manipulation often fall short in bridging this gap. Highly articulated, human-like hands with serial kinematic chains place actuators within the fingers or palm, leading to high distal mass and inertia, which compromises speed and payload [12], [13], [14]. Cable-driven systems mitigate this by relocating actuators to the forearm, but they introduce issues of cable friction, stretching, and durability, often resulting in lower transmission efficiency and reduced load capacity [15], [16], [17]. Simple, robust grippers [18], like commercial products from Robotiq [19], Schunk [20], and prototypes from research community [1], [10], [21] are suitable for standard industrial applications like pick-and-place, but lack the DoFs needed for in-hand manipulation and tool-based manipulation tasks.

Parallel kinematic mechanisms offer a powerful and promising solution to the design challenges of robotic manipulators. By actuating a single end-effector through multiple kinematic chains, these architectures inherently provide superior stiffness, improved load distribution, and enhanced

This work was supported by the Natural Science Foundation of Shanghai (Grant No. 25ZR1402370), and partially by Shanghai Frontiers Science Center of Human-centered Artificial Intelligence (ShangHAI), MoE Key Laboratory of Intelligent Perception and Human-Machine Collaboration (KLIP-HuMaCo). The experiments were supported by the Core Facility Platform of Computer Science and Communication, SIST, ShanghaiTech University.

R. Hu, Z. Zhu, Y. Leng, and C. Xiao are with the School of Information Science and Technology, ShanghaiTech University, Shanghai 201210, China. {hurz2024, zhuzhy1, lyt, xiaochx}@shanghaitech.edu.cn

J. Li and J. Liu are with Shanghai Fourier Intelligence Co., Ltd., Shanghai 201210, China. geek.men.0@gmail.com, sytuljs@163.com

†Contributed equally.

*Corresponding author: Chenxi Xiao.

Project webpage https://github.com/hurobomaster/TriCoSphere_hand

positional accuracy [22], [23], [24]. Moreover, locating actuators at a fixed base drastically reduces the moving inertia of the finger structure, enabling faster, more responsive motion. Despite these clear advantages, parallel kinematic designs, especially those with high degrees of freedom, remain relatively underexplored. While some existing efforts have investigated 2-DoF and 3-DoF configurations [9], [25], they frequently suffer from limited workspace volumes, and relatively lower finger DoFs than serial or cable-driven mechanisms, restricting their effectiveness for dexterous manipulation tasks [26], [27]. Unlocking the full potential of high-DoF parallel kinematic mechanisms is therefore a timely opportunity for advancing robotic hand design [28].

To bridge the aforementioned gaps, we present TriCoSphere, a novel manipulator architecture that leverages the advantages of parallel kinematics to deliver a fast, strong, and highly dexterous robotic hand (Fig. 1 and Fig. 2). Each of its three fingers is a 4-DoF Coaxial Spherical Parallel Mechanism (CSPM) [29]. This configuration pioneered for high-speed orienting tasks that simultaneously achieves a large range of motion, low inertia for rapid movements, and high load capacity through distributed actuation. By mounting all heavy actuators at the base, the distal mass is significantly reduced, addressing the inertia-related speed limitations often found in serial-link hands. The mechanism also offers a large workspace, as quantified through a derived kinematic model for manipulability analysis. Furthermore, we develop an efficient differential kinematics solver to enable motion control, allowing real-time control of each fingertip's position.

Extensive experiments demonstrate that TriCoSphere consistently achieves high performance across multiple metrics. Despite relying on low-cost, lightweight servo motors, the system attains a motion bandwidth of 6.5 Hz and supports a static payload of 4.1 kg per finger. For dexterity, the hand can perform in-hand manipulation tasks such as pivoting objects in-hand, and unscrewing a bottle cap or light bulb. In summary, the key contributions of this work are as follows:

- **Design of TriCoSphere:** A 12-DoF manipulator that includes three 4-DoF parallel-kinematic fingers, combining a large workspace with high speed and high payload capacity.
- **Kinematic Model:** A detailed kinematic analysis of the proposed CSPM, and the derived kinematics solver for real-time control.
- **Experimental Validation:** Extensive evaluation of payload capacity, motion speed, repeatability, and dexterity across a variety of grasping and in-hand manipulation tasks.

The design files and control software for the TriCoSphere are made open-source to contribute to further development in the robotics community.

II. RELATED WORK

A robotic manipulator's design is defined by its kinematic structure and actuation method, which together determine its capabilities. Research has explored a wide range of designs, balancing trade-offs among dexterity, speed, and payload.

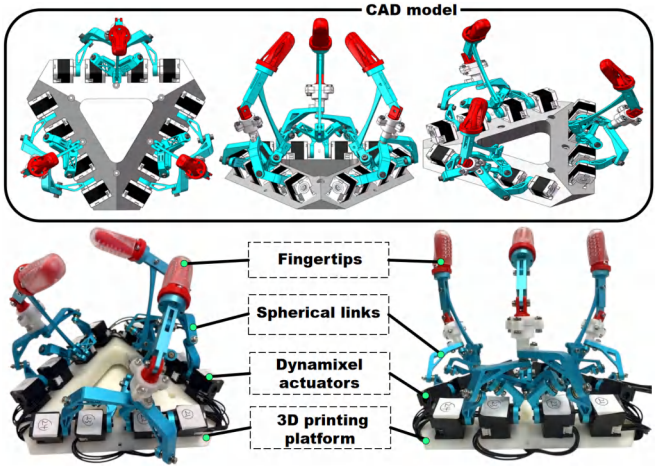

Fig. 2: Overview of the TriCoSphere Manipulator. The manipulator consists of three identical 4-DoF fingers symmetrically arranged around a central palm. All 12 actuators are located at the base, minimizing finger inertia.

A. Serial and Underactuated Manipulators

The majority of dexterous robotic hands are based on serial kinematics. Inspired by the human hand, highly articulated systems such as the HIT-DLR Hand [12], [13], employ a large number of direct-drive actuators to achieve high degrees of freedom. However, this approach increases weight, and results in large distal inertia, which limits both speed and force output.

To reduce complexity and cost, underactuated mechanisms have been widely adopted [10], [30], [31], [32]. Designs such as the Robotiq gripper [19], and the Yale OpenHand [33] use fewer actuators than DoFs, relying on passive elements to conformally grasp objects. While effective for grasping, underactuation sacrifices direct control over individual joints, limiting the ability to perform many tasks that require coordinated finger placements [4]. Another alternative is the tendon or cable-driven systems, which offer a compromise by relocating actuators away from the hand, as seen in systems like Shadow Hand [34], the Robonaut 2 Hand [35], and Utah/MIT dextrous hand [36]. This reduces finger inertia and enables faster motion [12]. However, such systems often face challenges from cable friction, stretch due to tensioning, and long-term wear, all of which can degrade control precision and load capacity [37].

B. Parallel Mechanisms in Manipulation

Parallel kinematic mechanisms (PKMs) offer an alternative design paradigm that can bridge this gap. With the Delta robot [24] as a canonical example, PKMs have been widely used in high-speed industrial pick-and-place tasks, achieving high stiffness, a superior payload-to-weight ratio, and high speed due to base-mounted actuators. PKMs have also been successfully employed in high-performance wrists, such as the Agile Eye, which provides rapid 3-DoF orientation for cameras [29], and in robotic hand wrists [23], [26], [38].

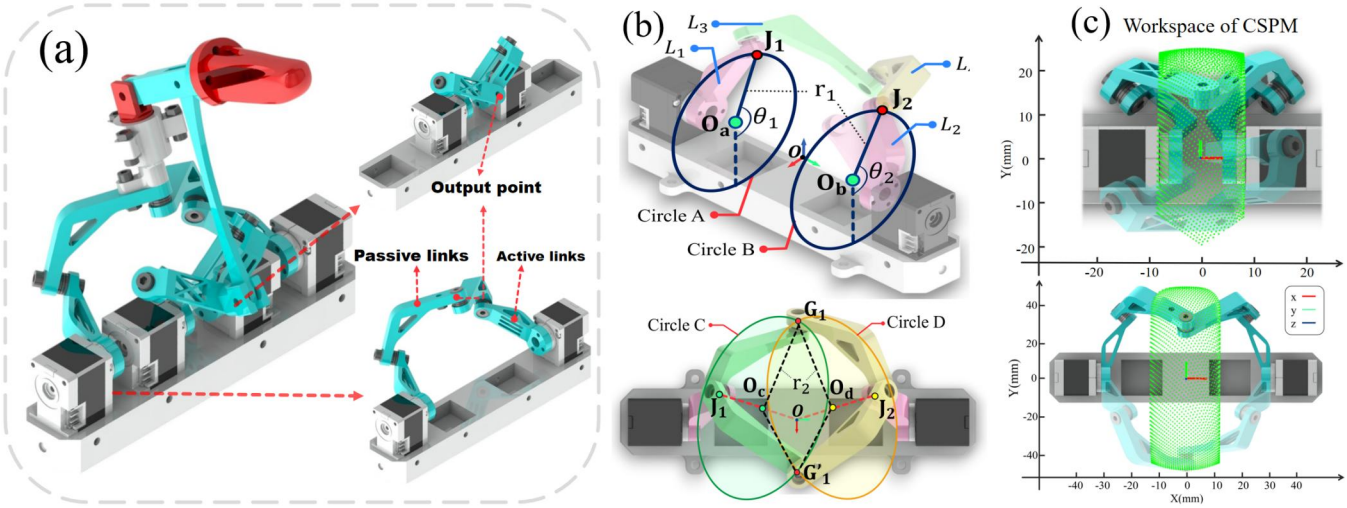

Fig. 3: Illustration of the single finger's mechanical structure based on CSPM. (a) The overall structure of a single finger, highlighting the two embedded CSPM mechanisms; the *active links* are directly driven by the actuators, while the *passive links* follow their motion within the closed-loop kinematic chain; (b) Joint trajectories of one CSPM mechanism; (c) Motion ranges of the first and second CSPM mechanisms, respectively.

Despite these benefits, the application of PKMs to multi-fingered dexterous hands remains uncommon. Some pioneering works have explored 3-DoF finger designs [9], but their degrees of freedom and available workspace volume are relatively limited compared to many serial mechanisms. Moreover, PKMs inherently face singularities that compromise grasp stability, which mainly stems from their closed-loop nature [39], [40]. In this work, we build upon the promise of parallel kinematics while addressing these limitations. We propose a novel 4-DoF finger design based on a Coaxial Spherical Parallel Mechanism (CSPM). This architecture expands the operational workspace and number of degrees of freedom compared to prior parallel finger designs [9], which improves dexterity and preserves PKM's advantages of high speed, stiffness, and payload capacity.

III. Methodology

A. Overview of Manipulator Design

The TriCoSphere manipulator comprises three identical robotic fingers symmetrically mounted around a circular base at 120° intervals (Fig. 2). Each finger is a 4-DoF Coaxial Spherical Parallel Mechanism (CSPM) with all joint actuators coaxially aligned at the base. This configuration offers two key advantages. First, apart from the base-mounted motors, each finger consists solely of passive linkages. In our design, the motion is initiated by *active links* directly coupled to the motor shafts, which then drive the remaining *passive linkages* within the closed-loop CSPM structure. This results in a lightweight structure with minimal moving mass and reduced inertia, thus enabling fast, responsive fingertip motion. Second, the parallel linkage distributes the load across multiple actuators. This improves payload capacity compared to traditional serial mechanisms where chained actuators bear the load sequentially.

B. Finger Kinematics

First, this paper presents the working principle of the TriCoSphere manipulator. We begin this with an analysis of the kinematics of each finger. As shown in Fig. 3 (a), each finger mechanism has four DoFs. The mechanism consists of two 2-DoF Coaxial Spherical Parallel Mechanisms (CSPMs), which together form the proximal phalanx, and a spatial five-bar linkage fingertip that is jointly actuated by the aforementioned CSPMs. The overall kinematic chain is determined by the coupled motion of these two components, with the corresponding kinematic models described below.

1) Design of CSPMs (proximal phalanges): The design of CSPM mechanism is shown in Fig. 3. This 2-DoF mechanism is a spatial five-bar linkage whose end-effector moves along a virtual spherical surface. The positions of joints $\mathbf{J_1}$ and $\mathbf{J_2}$ in the world coordinate frame are determined by the following kinematic equations:

$$\mathbf{J_1} = (-r_1, -r_1 \sin\theta_1, -r_1 \cos\theta_1), \tag{1}$$

$$\mathbf{J_2} = (r_1, -r_1 \sin\theta_2, -r_1 \cos\theta_2), \tag{2}$$

where the symbols $r_1, r_2, \theta_1, \theta_2$ and the spherical centers $\mathbf{O_a}, \mathbf{O_b}, \mathbf{O_c}, \mathbf{O_d}$ are illustrated in Fig. 3 (b). In our implementation, the origins of the two coordinate frames are located at $\mathbf{O_a} = (-r_1, 0, 0)$ and $\mathbf{O_b} = (r_1, 0, 0)$ in the world coordinate system (unit: mm). This spacing can be adjusted to design CSPMs with different dimensions.

Next, given the joint positions $\mathbf{J_1}$ and $\mathbf{J_2}$ as described above, we determine the position of the end-effector joint $\mathbf{G_1}$ (i.e., the output of the first 2-DoF CSPM). The joint $\mathbf{G_1}$ moves along two intersecting circular trajectories, referred to as circles C and D, as illustrated in Fig. 3 (b). To characterize these trajectories, we analyze the motion of linkages L_3 and L_4, which are connected to $\mathbf{J_1}$ and $\mathbf{J_2}$ via bearings and rotate

about the axes $\overrightarrow{\mathbf{OJ_1}}$ and $\overrightarrow{\mathbf{OJ_2}}$, respectively. Since all rotational axes pass through the origin $\mathbf{O}$, the vectors $\overrightarrow{\mathbf{OJ_1}}$ and $\overrightarrow{\mathbf{OJ_2}}$ serve as the normal vectors to the planes in which circles C and D lie. The radii of both circles, denoted by r_2 (the lengths of the segments $|\overrightarrow{\mathbf{O_cG_1}}|$ and $|\overrightarrow{\mathbf{O_dG_1}}|$) are determined by the geometry of links L_3 and L_4. The centers of circles C and D, denoted by $\mathbf{O_c}$ and $\mathbf{O_d}$ respectively, are given by:

$$\mathbf{O_c} = \frac{|\overrightarrow{\mathbf{OJ_1}}| - |\overrightarrow{\mathbf{O_cJ_1}}|}{|\overrightarrow{\mathbf{OJ_1}}|} \cdot (-r_1, -r_1 \sin\theta_1, -r_1 \cos\theta_1) \tag{3}$$

$$\mathbf{O_d} = \frac{|\overrightarrow{\mathbf{OJ_2}}| - |\overrightarrow{\mathbf{O_dJ_2}}|}{|\overrightarrow{\mathbf{OJ_2}}|} \cdot (r_1, -r_1 \sin\theta_2, -r_1 \cos\theta_2) \tag{4}$$

The position of $\mathbf{G_1}$ can then be determined as the intersection of the two circles, by solving the following constraint systems:

$$\begin{cases} \overrightarrow{\mathbf{OJ_1}} \cdot (\mathbf{G_1} - \mathbf{O_c}) = 0 \\ |\mathbf{G_1} - \mathbf{O_c}|^2 = r_2^2 \end{cases} \tag{5}$$

$$\begin{cases} \overrightarrow{\mathbf{OJ_2}} \cdot (\mathbf{G_1} - \mathbf{O_d}) = 0 \\ |\mathbf{G_1} - \mathbf{O_d}|^2 = r_2^2 \end{cases} \tag{6}$$

Solving the four equations from the systems Eq. (5) and (6) simultaneously forms a non-linear problem for deriving the coordinates of $\mathbf{G_1} = (\mathbf{G_{1x}}, \mathbf{G_{1y}}, \mathbf{G_{1z}})$. The forward kinematics solution, defined by the motor shaft angles (θ_1, θ_2), is given by:

$$\mathbf{G_{1z}} = \frac{-B \pm \sqrt{B^2 - 4AC}}{2A} \tag{7}$$

$$\mathbf{G_{1x}} = \frac{s_-(d - c_- \mathbf{G_{1z}})}{s_+ - c_-} \tag{8}$$

$$\mathbf{G_{1y}} = \frac{d - \cos\theta_1 \mathbf{G_{1z}} - \mathbf{G_{1x}}}{\sin\theta_1} \tag{9}$$

where the following auxiliary variables are used for brevity:

$$s_\mp = \frac{\sin\theta_1 \mp \sin\theta_2}{2}, \quad c_\mp = \frac{\cos\theta_1 \mp \cos\theta_2}{2},$$

$$d = r_1\alpha(1 + \sin\theta_1 + \cos\theta_1), \quad \text{with} \quad \alpha = 1 - \frac{|\overrightarrow{\mathbf{O_cJ_1}}|}{r_1\sqrt{2}}.$$

The coefficients A, B, C in $\mathbf{G_{1z}}$ can be obtained by substituting (8) and (9) into the circle constraint equation $|\vec{\mathbf{G}}_1 - \vec{\mathbf{O}}_c|^2 = r_2^2$. Their analytical forms are omitted here due to their length but are available in our code implementation.

Similarly, the end-effector position of the second CSPM can be derived using the same procedure. It is denoted as $\mathbf{G_2}$ and is characterized by the motor shaft angles θ_3 and θ_4.

By combining Eq. (7) and Fig. 3 (b), it can be observed that for the same servo angle combination, a single CSPM mechanism has two possible solutions for the end-effector position. Therefore, when two CSPM mechanisms are combined, four distinct solutions can be obtained for achieving the same end-effector configuration. Considering practical mechanical interference between linkages, the selected configuration is shown in Fig. 3 (a).

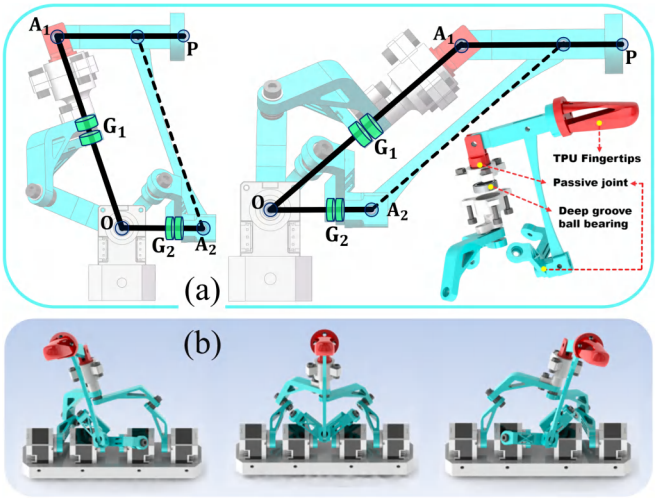

Fig. 4: Fingertip mechanism: (a) Side view of the five-bar linkage mechanism, and illustration of the fingertip's translational motion; (b) Demonstration of the lateral swinging motion of the fingertip mechanism.

2) Design of Fingertip Distal Mechanism: The fingertip mechanism is implemented as a five-bar linkage driven by two 2-DoF CSPMs, $\mathbf{G_1}$ and $\mathbf{G_2}$, as shown in Fig. 4. In our design, the output linkage is designed as a parallelogram to enhance in-plane stiffness and simplify kinematic analysis, allowing the fingertip position $\mathbf{P}$ to be directly defined by the expression in Eq. (10).

Kinematically, the output mechanism can be regarded as a spatial parallelogram with a fixed vertex at the origin $\mathbf{O}$, as shown in Fig. 4. The orientations of the two active links of the parallelogram, $\overrightarrow{\mathbf{OA_1}}$ and $\overrightarrow{\mathbf{OA_2}}$, are dictated by $\mathbf{G_1}$ and $\mathbf{G_2}$, respectively. These two links are independently controlled by their corresponding CSPM mechanisms. This configuration enables the working plane of the mechanism to perform a certain range of lateral swing, while also endowing the end-effector with the ability to reach the same target position with multiple orientations. Such flexibility afforded by this kinematic redundancy enhances the hand's adaptability for grasping diverse objects, as demonstrated in the subsequent experimental section and the supplementary video.

$$\overrightarrow{\mathbf{OP}} = \frac{\overrightarrow{\mathbf{OG_1}}}{|\overrightarrow{\mathbf{OG_1}}|}|\overrightarrow{\mathbf{OA_1}}| + \frac{\overrightarrow{\mathbf{OG_2}}}{|\overrightarrow{\mathbf{OG_2}}|}|\overrightarrow{\mathbf{A_1P}}| \tag{10}$$

3) Differential Inverse Kinematics: The overall kinematics of the finger are constructed by chaining the forward kinematics of the proximal and distal phalanges (i.e., CSPM and planar five-bar linkage). Based on this model, inverse kinematics is solved using a differential approach. Specifically, the Jacobian matrix is computed as $J = \frac{\partial \vec{\mathbf{P}}}{\partial \theta}$, where θ denotes the joint angles and $\vec{\mathbf{P}}$ is the fingertip position.

Given a desired fingertip velocity $\dot{\vec{\mathbf{P}}}$, the corresponding joint velocities $\dot{\theta}$ are obtained by:

$$\dot{\vec{\mathbf{P}}} = J\dot{\theta}, \quad \Rightarrow \quad \dot{\theta} = J^\dagger \dot{\vec{\mathbf{P}}} \tag{11}$$

where $J^\dagger$ denotes the Moore-Penrose pseudo-inverse of J.

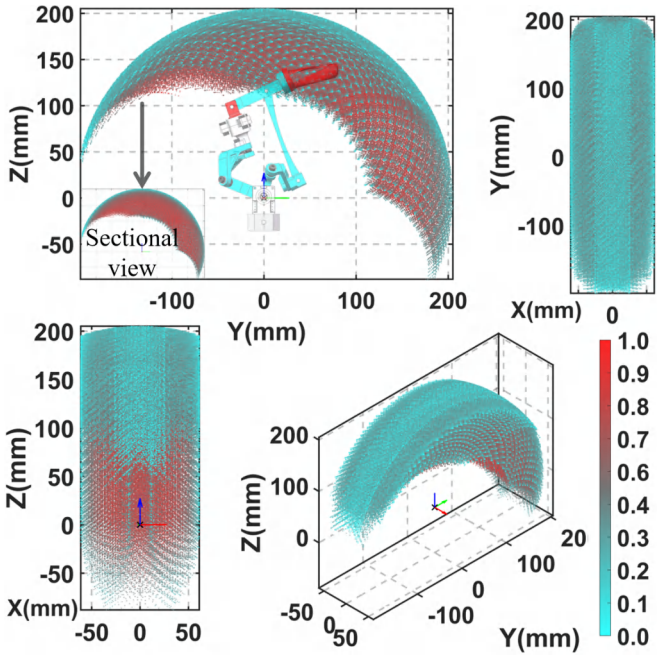

Fig. 5: Workspace and manipulability of a single finger: The finger's workspace shown from multiple perspectives, with manipulability represented by a color gradient ranging from blue (low) to red (high).

Dynamic Performance. The dynamic responsiveness of a finger was evaluated through frequency response analysis by commanding a sinusoidal trajectory and recording both the input and resulting positions. The system exhibited a closed-loop position-control bandwidth of 6.5 Hz (-3 dB), made possible by the low-inertia design with base-mounted actuators. The resulting rapid and agile movements are further demonstrated in the in-hand manipulation tasks.

C. Analysis of Hand's Dexterity

The workspace of an individual TriCoSphere finger is shown in Fig. 5. Further, we calculate the manipulability of the gripper to identify potential singular configurations. The manipulability index $\mathscr{M}$ quantifies the ability of the manipulator to generate motion in arbitrary directions within the workspace, which is defined as the square root of the determinant of the matrix $J^T J$ [41], where J is the Jacobian matrix. Singularities occur when $\mathscr{M}$ is zero.

$$\mathscr{M} = \sqrt{\det(JJ^T)} \tag{12}$$

The calculation results are shown in Fig. 5, the manipulability reaches its maximum in the central region of the workspace. Besides, no singular points are observed within the workspace except for the boundary.

D. Actuation System

To physically actuate the manipulator, we designed a control system for the proposed TriCoSphere. The system employs XC330-M288-T motors (Dynamixel Inc.), which supports both torque output and positional feedback. All XC330-M288-T units are connected via UART to a U2D2 hub, operating at a baud rate of 2 MHz.

A custom flange is 3D-printed to mount the TriCoSphere onto an XArm 6 collaborative robotic platform (UFactory Inc.). A host control computer manages the entire system, coordinating both the TriCoSphere and the XArm 6. A Python-based server program was developed to compute the TriCoSphere's forward and inverse kinematics in real time.

IV. Experiments

To validate the design and performance of the TriCoSphere manipulator, we conducted a series of experiments to characterize its payload capacity, repeatability, dynamic performance, and dexterity in manipulation tasks.

A. Payload Capacity and Repeatability

Payload Capacity. We evaluated the static payload capacity of the proposed CSPM. A weight was suspended from the fingertip until motor stall. As shown in Fig. 7 (c), each finger can reliably support a load of 4.1 kg.

Repeatability. The positioning repeatability of a single fingertip was measured using a dial gauge. The finger moved back and forth between two given target points for 30 cycles, with the end-effector's positions recorded at the end of each cycle. The standard deviation of the recorded positions was then calculated. The TriCoSphere finger achieved a repeatability of 0.0390 mm (standard deviation) and a maximum deviation of 0.1117 mm, demonstrating the accuracy provided by the parallel rigid linkage structure and the differential inverse kinematics controller.

B. Dexterity and Dynamic Performance

In-Hand Manipulation. The equal-interval placement of its three fingers, and also high-DoF design of fingers, makes TriCoSphere suited for in-hand manipulation. We validated this capability with a practical task of screwing a light bulb into its socket (Fig. 8, and supplementary video). The task requires all fingers to firmly hold the bulb while applying a coordinated twisting motion, followed by controlled release from the light bulb's surface. This motion is repeated until the bulb is fully seated in its socket. A single rotation cycle takes approximately 0.185 seconds on average, with no significant slip observed, highlighting the manipulator's high dynamic performance across a large range of motion.

Grasping Range and Versatility. To showcase the dexterity and large workspace of the TriCoSphere, we commanded the manipulator to grasp objects of varying sizes and shapes. As shown in Fig. 6, it successfully executed stable grasps on twelve everyday objects, ranging from a small 20 mm diameter cherry to a large 300 mm diameter acrylic sphere. The manipulator also demonstrated the ability to handle irregularly shaped items such as a glue tube, green pepper, and grape, as well as soft and fragile objects (shown in the video). These successful grasps demonstrate TriCoSphere's versatility and adaptability across diverse object types.

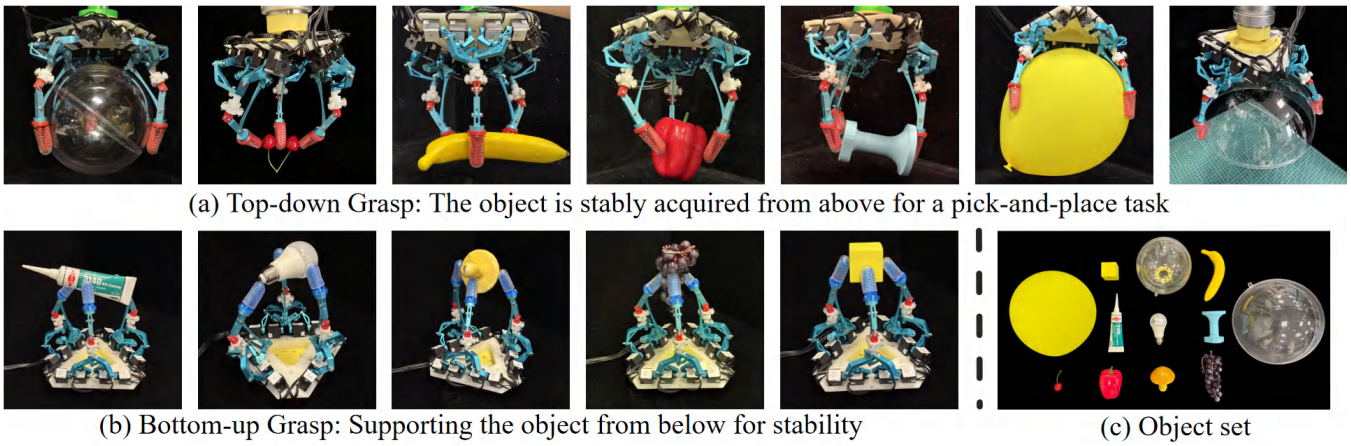

Fig. 6: Demonstration of the TriCoSphere's versatile grasping capabilities. The gripper successfully grasps 12 distinct objects, with sizes spanning from 20 mm to 300 mm. (a) Top-down and (b) bottom-up grasps. (c) The object set is diverse, including rigid, fragile, and deformable items: 200 mm acrylic sphere, cherry, banana, red bell pepper, irregularly-shaped 3D-printed part, big balloon, 300 mm acrylic hemisphere, glue bottle, lightbulb, mushroom, grapes, and small yellow cube.

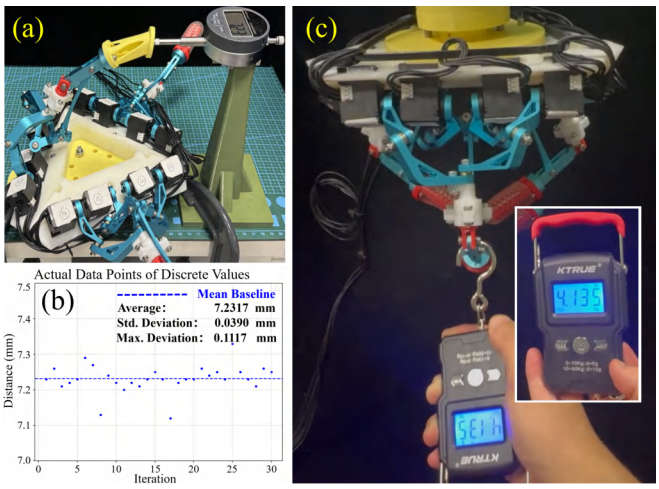

Fig. 7: Payload and repeatability characterization of the TriCoSphere manipulator. (a) Repeatability test setup using a dial gauge. (b) Distribution of repeatability test data across 30 cycles. (c) Payload test of a single finger, where the base was rigidly anchored to a fixed platform, demonstrating the capacity to withstand a 4.1 kg pulling force without motor stalling.

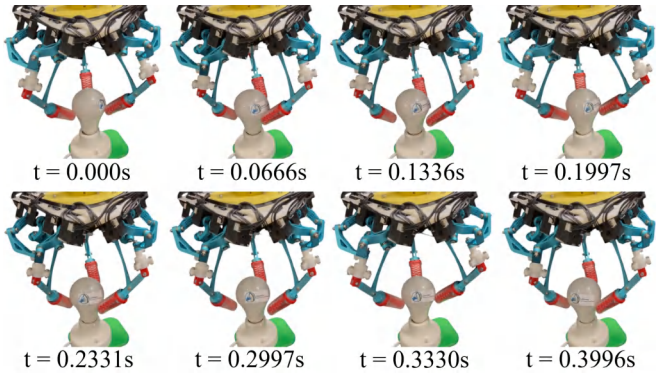

Fig. 8: Evaluation of the TriCoSphere manipulator's dynamic performance. The manipulator twisted the bulb 54 times within 10 seconds, demonstrating its high-speed capability.

C. Discussions

The experimental results showcase that the TriCoSphere manipulator effectively balances dexterity, speed, and payload objectives. Specifically, the CSPM design enables a high payload capacity using low-power motors of only 0.52 Nm and 103 rev/min, outperforming many serial-link or tendon-driven hands that rely on higher-power actuators [12], [13]. The measured 6.5 Hz bandwidth demonstrates dynamic performance on par with specialized high-speed grippers [24], while the 12-DoF architecture provides the dexterity required for grasping objects of diverse shapes and in-hand manipulation tasks.

The TriCoSphere is both cost-effective and simple to assemble. The prototype expenses ($840) come from CNC-machined aluminum components, estimated at $500, and 12 actuators which total approximately $340. As an alternative, 3D-printed parts can be used to further reduce costs, albeit at slight expense of motion repeatability and payload capacity. Additional costs for fasteners, bearings, and other miscellaneous hardware are minimal. The assembly of TriCoSphere is simple, which requires approximately two hours.

One limitation of the current prototype is its relatively large size, primarily resulting from the use of commercially available actuators that are not optimized for compact integration. Besides, although the parallel kinematic architecture provides the high structural stiffness required for heavy payload handling and precise motion control, it lacks the intrinsic compliance necessary for safe and adaptive interaction in unstructured, human-centric environments. Future work will focus on actuator miniaturization to achieve a more compact form factor, the integration of tactile sensing for enhanced perception and safety, and the extension of the system toward learning-based in-hand manipulation of heavy

and irregularly shaped objects.

V. Conclusions

In this paper, we introduced the TriCoSphere, a novel 12-DoF, 3-fingered robotic manipulator. The core of our design is the Coaxial Spherical Parallel Mechanism for each finger, which places all actuators at the base to achieve low inertia, high speed, and excellent load distribution. Furthermore, we developed its forward kinematic model and an efficient differential inverse kinematics solver to enable positional control of the fingertip.

Through comprehensive experiments and validations, we showcased the key advantages of the TriCoSphere. The manipulator demonstrated a payload capacity of 4.1 kg per finger, a high motion bandwidth of 6.5 Hz. Furthermore, its dexterity was confirmed through diverse manipulation tasks, including grasping objects from 20 mm to 300 mm and performing in-hand manipulation tasks including object reorientation via pivoting, and screwing a light bulb.

Future work will focus on integrating tactile sensing into the fingertips to enable active compliance and closed-loop force control, ensuring safer interactions and more robust grasping of unseen objects. We also plan to develop learning-based control policies to automate complex manipulation skills.

VI. Acknowledgment

Runze Hu contributed to conceptualization, robot design, experiments, and writing. Zhengying Zhu and Yatao Leng contributed to workspace analysis and visualization. Jinyu Li and Jingshuai Liu contributed to robot's structural optimization. Chenxi Xiao contributed to conceptualization, method and experiment design, funding acquisition, project management, and manuscript proofreading.

References

[1] A. Dollar and R. Howe, "The highly adaptive sdm hand: Design and performance evaluation," *I. J. Robotic Res.*, vol. 29, pp. 585–597, 04 2010.

[2] B. Siciliano and O. Khatib, Eds., *Springer handbook of robotics*, 2nd ed. Cham: Springer, 2016.

[3] A. Bicchi, "Hands for dexterous manipulation and robust grasping: a difficult road toward simplicity," *IEEE Transactions on Robotics and Automation*, vol. 16, no. 6, pp. 652–662, 2000.

[4] A. Bicchi and V. Kumar, "Robotic grasping and contact: a review," in *Proceedings 2000 ICRA. Millennium Conference. IEEE International Conference on Robotics and Automation. Symposia Proceedings (Cat. No.00CH37065)*, vol. 1, 2000, pp. 348–353 vol.1.

[5] R. Kanno, P. H. Nguyen, J. Pinskier, D. Howard, S. Song, and M. Kovac, "Hybrid soft electrostatic metamaterial gripper for multi-surface, multi-object adaptation," in *2024 IEEE 7th International Conference on Soft Robotics (RoboSoft)*. IEEE, Apr. 2024, p. 851–857. [Online]. Available: http://dx.doi.org/10.1109/RoboSoft60065.2024.10522020

[6] R. Calandra, A. Owens, M. Upadhyaya, W. Yuan, J. Lin, E. H. Adelson, and S. Levine, "The feeling of success: Does touch sensing help predict grasp outcomes?" *arXiv preprint arXiv:1710.05512*, 2017.

[7] S. Sundaram, P. Kellnhofer, Y. Li, J.-Y. Zhu, A. Torralba, and W. Matusik, "Learning the signatures of the human grasp using a scalable tactile glove," *Nature*, vol. 569, no. 7758, pp. 698–702, 2019.

[8] A. A. Basheer, J. Chang, Y. Chen, D. Kim, and I. Soltani, "Krysalis hand: A lightweight, high-payload, 18-dof anthropomorphic end-effector for robotic learning and dexterous manipulation," *arXiv preprint arXiv:2504.12967*, 2025.

[9] U. Kim, D. Jung, H. Jeong, J. Park, H.-M. Jung, J. Cheong, H. R. Choi, H. Do, and C. Park, "Integrated linkage-driven dexterous anthropomorphic robotic hand," *Nature communications*, vol. 12, no. 1, p. 7177, 2021.

[10] L. U. Odhner, L. P. Jentoft, M. R. Claffee, N. Corson, Y. Tenzer, R. R. Ma, M. Buehler, R. Kohout, R. D. Howe, and A. M. Dollar, "A compliant, underactuated hand for robust manipulation," 2013. [Online]. Available: https://arxiv.org/abs/1301.4394

[11] J. Zhou, J. Huang, Q. Dou, P. Abbeel, and Y. Liu, "A dexterous and compliant (dexco) hand based on soft hydraulic actuation for human-inspired fine in-hand manipulation," *IEEE Transactions on Robotics*, vol. 41, pp. 666–686, 2025.

[12] H. Liu, K. Wu, P. Meusel, N. Seitz, G. Hirzinger, M. Jin, Y. Liu, S. Fan, T. Lan, and Z. Chen, "Multisensory five-finger dexterous hand: The dlr/hit hand ii," in *2008 IEEE/RSJ International Conference on Intelligent Robots and Systems*, 2008, pp. 3692–3697.

[13] J. Butterfass, G. Hirzinger, S. Knoch, and H. Liu, "Dlr's multisensory articulated hand. i. hard-and software architecture," in *Proceedings. 1998 IEEE International Conference on Robotics and Automation (Cat. No. 98CH36146)*, vol. 3. IEEE, 1998, pp. 2081–2086.

[14] F. Lotti, P. Tiezzi, G. Vassura, L. Biagiotti, G. Palli, and C. Melchiorri, "Development of ub hand 3: Early results," in *Proceedings of the 2005 IEEE International Conference on Robotics and Automation*, 2005, pp. 4488–4493.

[15] H. Bai, B. G. Lee, G. Yang, W. Shen, S. Qian, H. Zhang, J. Zhou, Z. Fang, T. Zheng, S. Yang *et al.*, "Unlocking the potential of cable-driven continuum robots: A comprehensive review and future directions," in *Actuators*, vol. 13, no. 2. MDPI, 2024, p. 52.

[16] S. Min and S. Yi, "Development of cable-driven anthropomorphic robot hand*," *IEEE Robotics and Automation Letters*, vol. 6, pp. 1176–1183, 2021. [Online]. Available: https://api.semanticscholar.org/CorpusID:231973006

[17] J. Xu, S. Li, H. Luo, H. Liu, X. Wang, W. Ding, and C. Xia, "Muxhand: A cable-driven dexterous robotic hand using time-division multiplexing motors," *arXiv preprint arXiv:2409.12455*, 2024.

[18] M. Wüthrich, F. Widmaier, F. Grimminger, J. Akpo, S. Joshi, V. Agrawal, B. Hammoud, M. Khadiv, M. Bogdanovic, V. Berenz, J. Viereck, M. Naveau, L. Righetti, B. Schölkopf, and S. Bauer, "Trifinger: An open-source robot for learning dexterity," 2021. [Online]. Available: https://arxiv.org/abs/2008.03596

[19] E. K. Raptis, A. C. Kapoutsis, and E. B. Kosmatopoulos, "Robotiq: Empowering mobile robots with human-level planning for real-world execution," 2025. [Online]. Available: https://arxiv.org/abs/2502.12862

[20] S. W. Ruehl, C. Parlitz, G. Heppner, A. Hermann, A. Roennau, and R. Dillmann, "Experimental evaluation of the schunk 5-finger gripping hand for grasping tasks," in *2014 IEEE International Conference on Robotics and Biomimetics (ROBIO 2014)*, 2014, pp. 2465–2470.

[21] Y.-J. Kim, H. Song, and C.-Y. Maeng, "Blt gripper: An adaptive gripper with active transition capability between precise pinch and compliant grasp," *IEEE Robotics and Automation Letters*, vol. 5, no. 4, pp. 5518–5525, 2020.

[22] H. Li, Z. Wang, M. Sun, Y. Bao, Z. Ling, H. Jiang, X. Ouyang, and H. Yang, "Design paradigm for human size manipulator with high payload, repeatability, and bandwidth," *IEEE/ASME Transactions on Mechatronics*, 2024.

[23] Z. Liang, B. Wang, Y. Song, T. Zhang, C. Xiang, and Y. Guan, "Design of a novel cable-driven 3-dof series-parallel wrist module for humanoid arms," in *2021 IEEE International Conference on Mechatronics and Automation (ICMA)*, 2021, pp. 709–714.

[24] L. Rey and R. Clavel, "The delta parallel robot," in *Parallel Kinematic Machines: Theoretical Aspects and Industrial Requirements*. Springer, 1999, pp. 401–417.

[25] S. Wu, X. Wu, C. Wang, J. Wang, and J. Zhou, "Design and analysis of a novel 3-dof planar parallel manipulator with two kinematic chains," *Mechanics Based Design of Structures and Machines*, vol. 52, no. 11, pp. 9178–9200, 2024.

[26] S. Bai, "Optimum design of spherical parallel manipulators for a prescribed workspace," *Mechanism and Machine Theory*, vol. 45, no. 2, pp. 200–211, 2010.

[27] A. Antonov, "Parallel-serial robotic manipulators: A review of architectures, applications, and methods of design and analysis," 2024.

[28] C. Gosselin, T. Laliberté, and A. Veillette, "Singularity-free kinematically redundant planar parallel mechanisms with unlimited rotational capability," *IEEE Transactions on Robotics*, vol. 31, no. 2, pp. 457–467, 2015.

[29] C. Gosselin and J.-F. Hamel, "The agile eye: a high-performance three-degree-of-freedom camera-orienting device," in *Proceedings of the 1994 IEEE International Conference on Robotics and Automation*, 1994, pp. 781–786 vol.1.
[30] C. Luo, S. Yang, W. Zhang, Z. Ren, and J. Liang, "Mpj hand: A self-adaptive underactuated hand with flexible fingers of multiple passive joints," in *2016 International Conference on Advanced Robotics and Mechatronics (ICARM)*, 2016, pp. 184–189.
[31] G. Li, X. Liang, Y. Gao, T. Su, Z. Liu, and Z.-G. Hou, "A linkage-driven underactuated robotic hand for adaptive grasping and in-hand manipulation," *IEEE Transactions on Automation Science and Engineering*, vol. 21, no. 3, pp. 3039–3051, 2024.
[32] T. Laliberté, L. Birglen, and C. Gosselin, "'underactuation in robotic grasping hands'," *Japanese Journal of Machine Intelligence and Robotic Control*, vol. 4, pp. 77–87, 01 2002.
[33] R. Ma and A. Dollar, "Yale openhand project: Optimizing open-source hand designs for ease of fabrication and adoption," *IEEE Robotics & Automation Magazine*, vol. 24, no. 1, pp. 32–40, 2017.
[34] I. Akkaya, M. Andrychowicz, M. Chociej, M. Litwin, B. McGrew, A. Petron, A. Paino, M. Plappert, G. Powell, R. Ribas *et al.*, "Solving rubik's cube with a robot hand," *arXiv preprint arXiv:1910.07113*, 2019.
[35] C. Lovchik and M. Diftler, "The robonaut hand: a dexterous robot hand for space," in *Proceedings 1999 IEEE International Conference on Robotics and Automation (Cat. No.99CH36288C)*, vol. 2, 1999, pp. 907–912 vol.2.
[36] S. Jacobsen, E. Iversen, D. Knutti, R. Johnson, and K. Biggers, "Design of the utah/mit dextrous hand," in *Proceedings. 1986 IEEE International Conference on Robotics and Automation*, vol. 3. IEEE, 1986, pp. 1520–1532.
[37] J. Butterfass, M. Grebenstein, H. Liu, and G. Hirzinger, "Dlr-hand ii: next generation of a dextrous robot hand," in *Proceedings 2001 ICRA. IEEE International Conference on Robotics and Automation (Cat. No.01CH37164)*, vol. 1, 2001, pp. 109–114 vol.1.
[38] R. Di Gregorio, "Design of novel human wrist prostheses based on parallel architectures: Dimensional synthesis and kinetostatics," *Biomimetics*, vol. 10, no. 1, 2025. [Online]. Available: https://www.mdpi.com/2313-7673/10/1/44
[39] C. Gosselin, J. Angeles *et al.*, "Singularity analysis of closed-loop kinematic chains." *IEEE transactions on robotics and automation*, vol. 6, no. 3, pp. 281–290, 1990.
[40] H. D. Taghirad, *Parallel robots: mechanics and control*. CRC press, 2025.
[41] T. Yoshikawa, "Manipulability of robotic mechanisms," *The international journal of Robotics Research*, vol. 4, no. 2, pp. 3–9, 1985.